# Indirect generation of quadrupole polaritons from dark excitons in $Cu_2O$

J. I. Jang,* Y. Sun, and J. B. Ketterson†
*Department of Physics and Astronomy, Northwestern University, 2145 Sheridan Road, Evanston, Illinois 60208, USA*
(Received 28 June 2007; revised manuscript received 14 September 2007; published 14 February 2008)

The momentum-dependent electron-hole exchange interaction splits the triply degenerate orthoexcitons into the bright and dark states in $Cu_2O$, depending on the direction of **k** inside the crystal. Employing resonant two-photon excitation along a (100) direction at 2 K, we selectively create the dark orthoexcitons that do not couple to the radiation field. However, these excitons can radiatively recombine due to subsequent conversion into the bright states. By measuring the polarization dependence, we find that the two bright states are equally populated due to cross relaxation. We also find that this bright orthoexciton luminescence is highly directional and well aligned with the initial laser propagating direction. This strongly indicates that propagating quadrupole orthoexciton-polaritons, which are the quantum superposition of bright orthoexcitons and photons, are indirectly generated. We find that the dark-to-bright relaxation mechanism can be significantly affected in the presence of hot excitons due to density-dependent scattering.

DOI: 10.1103/PhysRevB.77.075201 PACS number(s): 71.35.−y, 71.36.+c, 78.55.−m

## I. INTRODUCTION

Cuprous oxide ($Cu_2O$, also called cuprite) is a direct gap semiconductor with a band gap of 2173 meV; electron-hole (e-h) pairs excited across this band gap exhibit a Rydberg series of exciton states.[1] The (yellow) exciton in this material consists of an electron in the lowest conduction band ($^2\Gamma_6^+$) and a hole in the highest valence band ($^2\Gamma_7^+$), both having only simple spin degeneracy. The fourfold spin-degenerate 1*s* exciton state is split by the *momentum-independent* exchange interaction into a triply degenerate orthoexciton ($^3\Gamma_{25}^+$) and a nondegenerate paraexciton ($^1\Gamma_2^+$) with an energy splitting of $\Delta=12$ meV. The orthoexciton state is further split by the so-called $k^2$-dependent exchange interactions, which are on the scale of several $\mu$eV.[2,3] For example, along a (100) direction, the triply degenerate state splits into the nondegenerate dark orthoexciton ($|O_{yz}\rangle$) and the doubly degenerate bright orthoexciton ($|O_{xy}\rangle$ and $|O_{zx}\rangle$). Both dark and bright orthoexcitons can recombine via indirect phonon-assisted processes, but only the bright states can radiatively recombine by a quadrupole-allowed *direct transition*, as illustrated in Table I.

Near the light cone ($k \simeq 2.63\times10^5$ cm$^{-1}$), a bright orthoexciton quadrupole couples to the electromagnetic field, resulting in an orthoexciton-polariton. This is a quantum coherent superposition of a bright orthoexciton (matter) and a photon (light) field. The propagating nature of the orthoexciton-polariton was first observed in the variation of the beat period using coherent quantum beat spectroscopy under resonant one-photon excitation.[4] By contrast, a dark orthoexciton does not directly couple to the radiation field, and therefore, a direct creation of dark orthoexcitons is not allowed under one-photon excitation (see Table I). Since both excitonic matter species are generated under resonant excitation, the initial coherence of the laser light is essentially carried by them. The total coherence time of orthoexciton-polaritons or dark orthoexcitons is basically limited by various elastic and inelastic dephasing processes,[5] and crucially depends on the local impurity concentration.[6] Both dark orthoexcitons and orthoexciton-polaritons are potentially important in semiconductor-based quantum information science.[7] In this work, we employ resonant two-photon excitation in order to initially generate *dark orthoexcitions* and study their subsequent conversion into the "propagating" bright states.

## II. EXPERIMENTAL METHODS

Our experiments were performed on a natural-growth $Cu_2O$ crystal cut with all (100) faces ($0.8\times1.3\times1.9$ mm$^3$). The sample was immersed in superfluid helium in an optical cryostat and oriented at $\theta=45°$ relative to the polarization direction of the laser (see Fig. 3 inset), ensuring the maximum two-photon excitation of dark orthoexcitons. The corresponding $\theta$ dependences of the two-photon selection rules[8] are shown in Table I, which is consistent with our observations (see Fig. 3).

A schematic diagram of the experimental setup is depicted in Fig. 1. The frequency-tripled output of a mode-locked Nd:YAG (where YAG denotes yttrium aluminum garnet) laser pumps an optical parametric amplifier (OPA) tuned to the two-photon resonance energy $\varepsilon_{2p}=\hbar\omega_{2p}=1016.48$ meV (1219.4 nm). The laser pulse from the OPA is vertically polarized with a pulse width of about 15 ps and a repetition rate of 10 Hz. The incident laser pulse is weakly focused as a spot 500 $\mu$m in diameter using a 15 cm focal-length lens. The corresponding incident power flux is about 310 MW/cm$^2$. The photoluminescence (PL) is collected in the transmission geometry from the opposite surface of the sample and focused onto a fiber optic bundle mounted on a goniometer, allowing us to measure the angular dependence

TABLE I. Selection rules for a (100) direction.

| Eigenstate | One-photon | Two-photon |
|---|---|---|
| $\|O_{xy}\rangle$ | $\cos^2\theta$ | 0 |
| $\|O_{yz}\rangle$ | 0 | $\sin^2 2\theta$ |
| $\|O_{zx}\rangle$ | $\sin^2\theta$ | 0 |

 

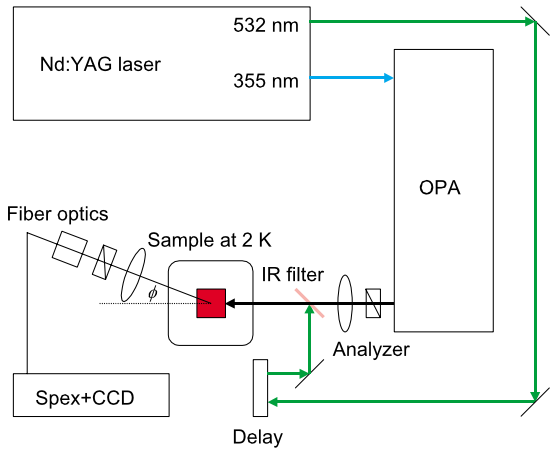


FIG. 1. (Color online) Schematic diagram of the experimental setup. Here, $\phi$ is the angle between the laser beam and the collection direction of the luminescence.

($\phi$) of the PL. The output of the fiber optic bundle is coupled to the entrance slit of a Spex Spec-One 500 M spectrometer and detected using a liquid nitrogen cooled CCD camera.

In order to observe scattering between the initially generated dark orthoexcitons and hot excitons, we use the frequency-doubled output of the Nd:YAG laser which was synchronized with the OPA pulse using appropriate delays. A dichroic mirror is used an effective IR filter, allowing simultaneous excitation from the two beam sources. In order to verify the one- and two-photon selection rules, a pair of analyzers is placed in front of and behind the sample. The collection efficiency of our optical system as a function of $\phi$ is explained in Ref. 6.

## III. PHOTOLUMINESCENCE AT 2 K AND INDIRECT GENERATION OF ORTHOEXCITON-POLARITONS

Figure 2 shows a typical time-integrated PL spectrum obtained at 2 K and $\phi=0°$. Considering that *optically inactive* dark orthoexcitons are initially generated in our excitation geometry, it seems rather surprising to observe several luminescence lines. Once created, however, these excitons undergo various relaxation processes and can recombine accompanied with the emission of a single photon. For example, they can (i) inelastically scatter from optical phonons, causing the phonon replica ($X_o-\Gamma_{12}^-$); (ii) be captured by ambient impurities, where the symmetry of an exciton is broken and the parent selection rule does not apply, resulting in the broad bound exciton luminescence;[9] and (iii) convert into the bright orthoexciton states that directly recombine, yielding the sharp $X_o$ line. They also can either nonradiatively decay due to phonon cascade or down-convert into the lower-lying paraexcitons by emitting a single TA phonon.[10] Compared with other inelastic energy relaxation processes that cause irreversible damping of dark orthoexcitons, we find that the conversion into the bright state is the most dominant mechanism based on a strong $X_o$ luminescence.

In order to verify that the direct $X_o$ line arises from two bright states that are subsequently converted from the dark

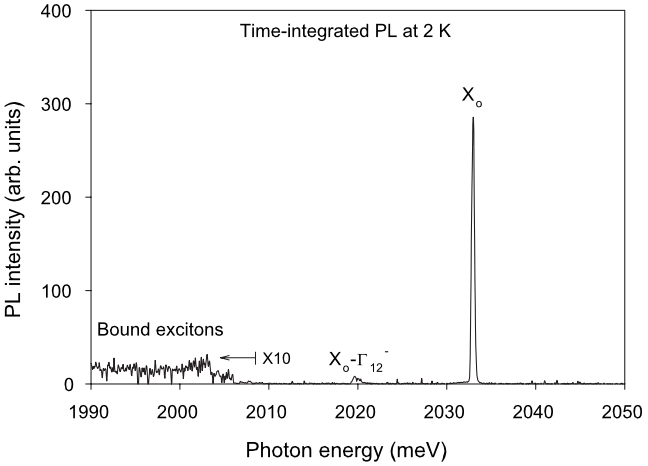


FIG. 2. Time-integrated PL spectrum at 2 K and $\phi=0°$ under two-photon excitation along a (100) direction that initially creates dark orthoexcitons. The direct line and $\Gamma_{12}^-$ optical phonon replica are denoted by $X_o$ and $X_o-\Gamma_{12}^-$, respectively. The observed phonon replica is well explained by a Boltzmann distribution with a gas temperature slightly higher than 2 K. A broad continuum below 2010 meV corresponds to the bound exciton luminescence (10× magnified).

state, we confirmed the one- and two-photon selection rules using two analyzers. The dots in Fig. 3 correspond to the observed two-photon selection rules for dark orthoexcitons inferred from the bright-state luminescence ($X_o$ line). Considering that the sample orientation is 45° and the analyzer is in front of the sample, the overall two-photon polarization dependence is shown as the solid curve and is given by

$$P_{2p} \propto \sin^2[2(\theta - 45°)]\cos^4\theta, \tag{1}$$

where the extra $\cos^4\theta$ term arises from *two-photon* excita-

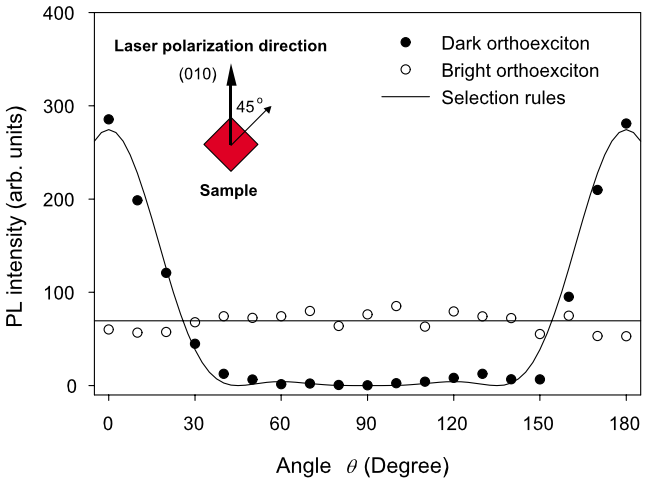


FIG. 3. (Color online) The dots (circles) correspond to the observed polarization dependence of the $X_o$ line obtained using analyzers in front of (behind) the sample. Superimposed solid curve (line) represents the two-photon (one-photon) selection rules. The inset schematically shows our excitation geometry.

tion of the incident laser intensity that decreases with $\cos^2\theta$, as the analyzer rotates from $\theta=0°$.

The circles correspond to the observed one-photon selection rules for bright orthoexcitons, converted from dark orthoexcitons, obtained with the analyzer behind the sample. We find that the $X_o$ intensity barely depends on the analyzer angle. Considering the total polarization of the two bright states where $|O_{xy}\rangle \propto \cos^2\theta$ and $|O_{zx}\rangle \propto \sin^2\theta$, this implies that the two degenerate bright states are equally populated via the dark orthoexcitons:

$$P_{1p} = \text{const} \propto \sin^2\theta + \cos^2\theta. \tag{2}$$

We find that the observed one- and two-photon selection rules barely depend on the excitation power in our experimental range. Clearly, the observed polarization dependencies support the conclusion that the strong direct luminescence arises from dark-to-bright conversion.

This dark-to-bright conversion was first observed by Yoshioka and Kuwata-Gonokami under two-photon excitation along the (110) direction.[7] The measured conversion rate is about 5 $ns^{-1}$. The contribution to this conversion rate due to phonon scattering can be estimated by the deformation potential theory. It is well known that simple hydrostatic compression (scalar) does not induce state mixing among three different orthoexciton states. Instead, the phonon-mediated transition among "different" orthoexciton states must arise from the off-diagonal shear tensor due to a single TA-phonon emission.[11] The associated shear deformation potential is given by

$$\Xi_{shear} = \left(\frac{8}{15}\Xi_{zz}^2 + \frac{1}{2}\Xi_{xy}^2\right)^{1/2}, \tag{3}$$

where $\Xi_{zz}=-0.29$ eV and $\Xi_{xy}=0.18$ eV.[12–14] In Eq. (3), only the second term causes transitions between dark and bright states, yielding a conversion rate given by

$$\Gamma(T) = \frac{\Xi_{xy}^2 m^2 \delta}{3\pi\rho v_T \hbar^4}\left(1 + \frac{2k_B T}{v_T\sqrt{2m\delta}}\right), \tag{4}$$

where $m=2.7m_e$ is the exciton mass, $\rho=6.1$ g/cm$^3$ is the mass density of $Cu_2O$, and $v_T=1.3$ km/s is the TA-phonon velocity. With the measured splitting $\delta=2$ $\mu$eV along this direction,[2,3] Eq. (4) yields a conversion rate $\Gamma \simeq 0.7\times10^{-4}$ $ns^{-1}$ at 2 K. This implies that dark-to-bright conversion via phonon scattering is negligible at this temperature (see also Ref. 7).

This dark-to-bright conversion involves scattering into different orthoexciton states with negligible contribution from inelastic phonon scattering. Therefore, it most likely arises from state mixing caused not only by local strain fields or impurities, but also the so-called cross relaxation, where two dark $|O_{yz}\rangle$ states elastically scatter to *equally* populate two bright states of $|O_{xy}\rangle$ and $|O_{zx}\rangle$ by satisfying angular momentum conservation. Although the dark orthoexcitons lose their initial coherence due to pure dephasing processes,[7] this implies that their phase information can be partially carried by subsequently generated bright orthoexcitons, because elastic scattering only induces a phase shift in the total ensemble coherence.

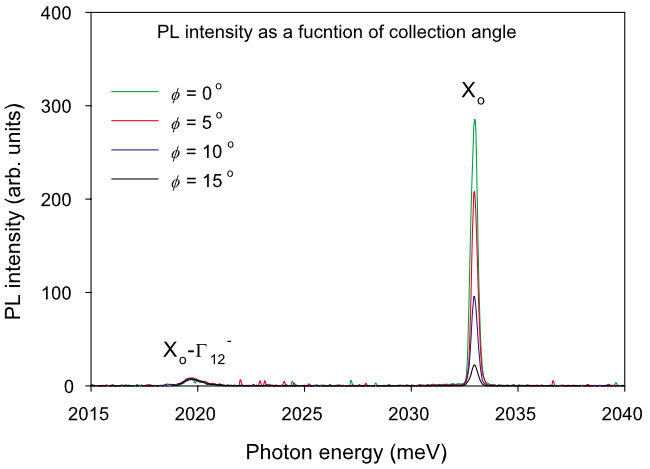


FIG. 4. (Color online) Time-integrated spectra at 2 K as a function of the collection angle $\phi=0°$, 5°, 10°, and 15°. The spectral features for the direct and phonon replica are explained in the text.

Figure 4 shows the PL spectra under the same conditions for several collection angles $\phi$ in the range of 0–15°. Each PL intensity is correctly scaled considering the collection efficiency of our optical system.[6] Note that the direct $X_o$-line PL intensity sharply depends on $\phi$ and is well correlated with the laser-propagation direction, whereas the indirect phonon line does not, i.e., it is essentially isotropic. This strongly indicates that the initial momentum of a dark orthoexciton inherited from the laser is nearly conserved after the conversion. This leads the momentum of a subsequently generated bright orthoexciton near the light cone to form an *orthoexciton-polariton*, which propagates along the initial laser direction.

This observation also makes the previously mentioned phonon-scattering mechanism unlikely, because inelastic phonon scattering can readily change the propagation direction of the dark orthoexcitons and their coherence arbitrarily, which must yield a rather isotropic $X_o$ line after conversion, just like the isotropic phonon replica $X_o-\Gamma_{12}^-$. Along with Fig. 3, this strong angular dependence of the $X_o$ line indicates that the initially created dark orthoexcitons convert into propagating orthoexciton-polaritons with minimal inelastic scattering. This fact implies that one can generate moving orthoexciton-polaritons either directly or indirectly using two-photon excitation, regardless of the crystal orientation.

## IV. DARK-TO-BRIGHT CONVERSION IN THE PRESENCE OF HOT EXCITONS

We now use the accompanying frequency-doubled 532 nm output of our Nd:YAG laser to examine the effect of hot excitons on dark-to-bright conversion. As shown in Fig. 1, the 532 nm laser does not pass through the focusing lens, and, therefore, is defocused and entirely covers the sample surface. This initially creates a dense gas of hot e-h pairs that quickly form hot excitons within 3 $\mu$m of the excited surface, which spread inside the crystal with rather fast diffusion coefficients.[15,16] Using the 30% quantum efficiency at

this wavelength,[16] the estimated initial density of hot excitons is about $10^{17}$ cm$^{-3}$.

The two-photon absorption length basically depends on the excitation-power flux, but the dark orthoexcitons are mostly generated at the excitation surface and their initial depth distribution rapidly decreases with the penetration depth [see, for example, Eq. (7) in Ref. 17]. Since two incident photons with a total momentum of $2(\hbar\omega_{2p}/c)$ from the OPA generate a dark orthoexciton, the initial velocity of a dark orthoexciton is given by $v=2(\hbar\omega_{2p}/mc)\simeq 0.44$ $\mu$m/ns, where $c$ is the velocity of the light and $m$ is the translational mass of an exciton, which is about 2.7 times larger than the electron mass. Assuming the measured time scale for dark-to-bright conversion of about 0.2 ns,[7] the maximum distance traveled by the dark orthoexciton cannot exceed 0.1 $\mu$m $\ll 3$ $\mu$m. This implies that initially created dark orthoexcitons near the surface are heavily affected by diffusive hot excitons in the presence of the secondary beam, and subsequently generated orthoexciton-polaritons travel most of the region of the crystal before escaping from it and converting into bare photons that we detect.

Figure 5 clearly demonstrates that dark-to-bright conversion is *severely interrupted* when hot excitons are present. In Fig. 5(a), the dots show the power dependence of the orthoexciton-polariton PL intensity for the two-photon excitation-power flux ranging from 10 to 540 MW/cm$^2$. Although the data points are rather scattered, we find that the observed $X_o$ intensity approximately increases quadratically with the excitation power for excitation levels smaller than 100 MW/cm$^2$ (see also Fig. 5 in Ref. 18). For excitation levels larger than 100 MW/cm$^2$, the $X_o$ intensity increases linearly with the excitation power, indicating that *nonradiative density-dependent* recombination starts to occur.[19] The circles represent the corresponding PL intensities under the same conditions but now in the presence of the secondary 532 nm beam, after subtracting the contribution from the 532 nm excitation beam itself. It is interesting that the (forward collected) $X_o$ PL intensities are significantly reduced in the presence of hot excitons. Also, note that the displacement between the dots and circles increases with the excitation-power flux. This indicates that the conversion into orthoexciton-polaritons is suppressed by *two-body* scattering between dark orthoexcitons and hot excitons. Obviously, collision with hot excitons induces thermalization of initially very cold dark orthoexcitons, shifting their momenta far from the polariton bottleneck. We find that the observed displacement decreases with the time delay between the OPA pulse and the frequency-doubled YAG pulse. For a delay of more than $\pm 1$ ns between the two pulses, no difference between the dots and circles in Fig. 5 is observed.

The above interpretation is further confirmed by using another sample polished along a (111) direction under the same conditions. This sample exhibits much stronger bound exciton luminescence.[9] For this direction, the two-photon selection rules do not depend on the polarization direction of the incident light and the corresponding excitation initially generates both orthoexciton-polaritons and dark orthoexcitons.[6] As shown in Fig. 5(b), the measured $X_o$ intensity from this sample at a given excitation level is about two times smaller, due to more enhanced impurity capture.

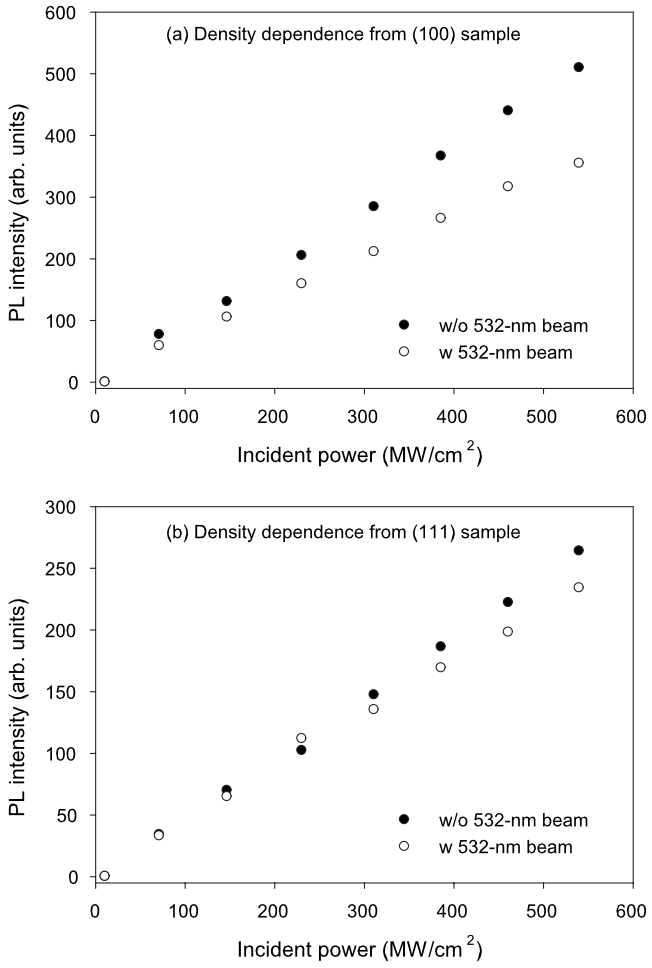


FIG. 5. (a) Dots show the measured orthoexciton-polariton PL ($X_o$) intensities for power fluxes from the OPA in the range from 10 to 540 MW/cm$^2$ at 2 K and $\phi=0°$. The circles correspond to the measured $X_o$ intensities arising from the OPA pulses in the presence of the secondary beam with the contribution from the latter subtracted. (b) Dots (circles) correspond to the measured $X_o$ intensities with and without the 532 nm beam under the same conditions obtained from a $Cu_2O$ sample polished along a (111) direction. The data indicate that dark-to-bright conversion can be significantly affected by hot excitons as explained in the text.

Particularly interesting is that the difference between the dots and circles is now noticeably reduced. This implies that hot exciton scattering is relatively unimportant for orthoexciton-polaritons compared with the case for dark orthoexcitons. This presumably arises from the fact that an orthoexciton-polariton, with an effective mass several orders of magnitude smaller, propagates rapidly with a group velocity[4] of the order of 100 times smaller than the speed of light, and quickly escapes the region where hot excitons reside. In contrast, the relatively very massive, and therefore slowly moving, dark orthoexcitons should have more chance to scatter with hot excitons. Therefore, the difference between dots and circles in Fig. 5(b) most likely arises from elastic scattering between partially created dark orthoexcitons and hot excitons.

In Fig. 6, we plot the corresponding angular distributions (dots) for the $X_o$ intensity obtained from our (100) sample at

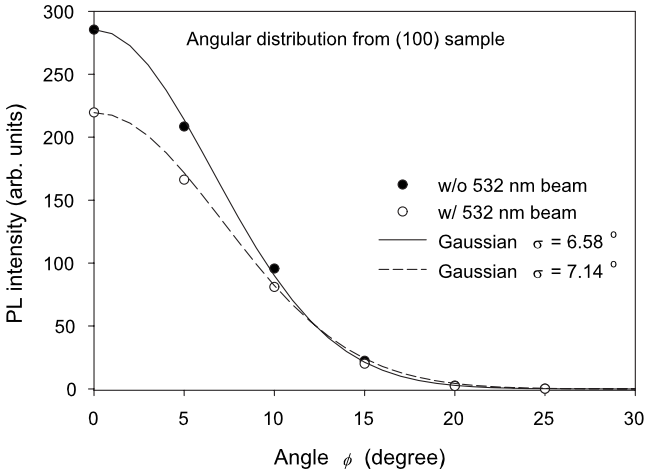


FIG. 6. Dots (circles) show the corresponding angular distribution of the $X_o$ intensities in the absence (presence) of the 532 nm beam under an incident photon density of 310 MW/cm$^2$ for several collection angles $\phi$. The superimposed curves are phenomenological Gaussian fits to the data.

310 MW/cm$^2$. The superimposed solid curve corresponds to an empirical Gaussian fit to the data with a standard deviation $\sigma$=6.58°. This angular distribution is significantly broader than the angular divergence of the laser light, and the origin of this broader angular distribution has been attributed to impurity scattering.[6] In the presence of the secondary beam, we find that the observed angular distribution (circles) becomes noticeably broader as indicated by a larger standard deviation $\sigma$=7.14° in the fit (dashed curve). This clearly arises from scattering by hot excitons that not only depopulates cold orthoexciton-polaritons through energy transfer, but also changes the initial propagation direction of orthoexciton-polaritons. The difference in the observed angular distributions again supports our thesis that dark-to-bright cross relaxation can be suppressed by hot exciton elastic scattering.

## V. SUMMARY AND CONCLUSIONS

In the present work, we have generated dark orthoexcitons in $Cu_2O$ and examined their key relaxation process experimentally. The observed strong direct luminescence ($X_o$) and its polarization dependence clearly indicate dark-to-bright conversion mostly due to cross relaxation. Since the mechanism does not involve any inelastic phonon scattering, the subsequently generated bright states are correlated with dark orthoexcitons and, therefore, the incident laser. This interpretation has been experimentally demonstrated by observing the collection angle dependence of the $X_o$ line, strongly indicating orthoexciton-polaritons propagating along the initial laser propagating direction. We have also experimentally shown that dark-orthoexciton to orthoexciton-polariton conversion can be significantly affected by the presence of hot excitons.

Unlike the direct creation of orthoexciton-polaritons via resonant one-photon excitation, the initially created excitonic matter under resonant two-photon excitation crucially depends on the sample orientation in this semiconductor. However, fast dark-to-bright conversion on a subnanosecond scale ensures that the direct PL line solely arises from indirectly generated orthoexciton-polaritons propagating through the medium, although dark orthoexcitons are initially generated. Our observations indicate that two-photon excitation in $Cu_2O$ eventually generates moving orthoexciton-polaritons regardless of the crystal orientation.

## ACKNOWLEDGMENTS

The authors would like to thank J. P. Wolfe at the University of Illinois for providing the sample used in this work. This work is supported by the National Science Foundation under a U.S./Ireland cooperation, Grant No. 0306731, and the Northwestern Materials Research Center under NSF Grant No. DMR-0520513.

*joonjang@uiuc.edu
†j-ketterson@northwestern.edu

[1] M. Hayashi and K. Katsuki, J. Phys. Soc. Jpn. **7**, 599 (1952).
[2] G. Dasbach, D. Fröhlich, H. Stolz, R. Klieber, D. Suter, and M. Bayer, Phys. Rev. Lett. **91**, 107401 (2003).
[3] G. Dasbach, D. Fröhlich, R. Klieber, D. Suter, M. Bayer, and H. Stolz, Phys. Rev. B **70**, 045206 (2004).
[4] D. Fröhlich, A. Kulik, B. Uebbing, A. Mysyrowicz, V. Langer, H. Stolz, and W. von der Osten, Phys. Rev. Lett. **67**, 2343 (1991).
[5] T. Takagahara, Phys. Rev. B **31**, 8171 (1985).
[6] J. I. Jang and J. B. Ketterson, Phys. Rev. B **76**, 155210 (2007).
[7] K. Yoshioka and M. Kuwata-Gonokami, Phys. Rev. B **73**, 081202(R) (2006).
[8] For general two-photon selection rules in a solid, see R. J. Elliot, Phys. Rev. **124**, 340 (1961); M. Inoue and Y. Toyozawa, J. Phys. Soc. Jpn. **20**, 363 (1965).
[9] J. I. Jang, Y. Sun, B. Watkins, and J. B. Ketterson, Phys. Rev. B **74**, 235204 (2006).
[10] J. I. Jang, K. E. O'Hara, and J. P. Wolfe, Phys. Rev. B **70**, 195205 (2004).
[11] J. I. Jang and J. P. Wolfe, Phys. Rev. B **73**, 075207 (2006).
[12] M. H. Manghani, W. S. Brower, and H. S. Parker, Phys. Status Solidi A **25**, 69 (1974).
[13] R. G. Waters, F. H. Pollak, R. H. Bruce, and H. Z. Cummins, Phys. Rev. B **21**, 1665 (1980).
[14] H.-R. Trebin, H. Z. Cummins, and J. L. Birman, Phys. Rev. B **23**, 597 (1981).
[15] D. P. Trauernicht and J. P. Wolfe, Phys. Rev. B **33**, 8506 (1986).
[16] K. E. O'Hara, J. R. Gullingsrud, and J. P. Wolfe, Phys. Rev. B **60**, 10872 (1999).
[17] K. E. O'Hara and J. P. Wolfe, Phys. Rev. B **62**, 12909 (2000).
[18] T. Goto, M. Y. Shen, S. Koyama, and T. Yokouchi, Phys. Rev. B **55**, 7609 (1997); **56**, 4284(E) (1997).
[19] J. I. Jang and J. P. Wolfe, Phys. Rev. B **72**, 241201(R) (2005); Solid State Commun. **137**, 91 (2006); Phys. Rev. B **74**, 045211 (2006).